Structural characterization of kerogen in 3.4 Ga Archaean cherts from the Pilbara Craton, Western Australia

Craig P. Marshall [a,b,*], Gordon D. Love [c,d,**], Colin E. Snape [e], Andrew C. Hill [f,b],
Abigail C. Allwood [b], Malcolm R. Walter [b], Martin J. Van Kranendonk [g,b],
Stephen A. Bowden,

profiles exist between HyPy products of Strelley Pool Chert kerogens and an oil-window-mature Mesoproterozoic kerogen from Roper Group (ca. 1.45 Ga), which is biogenic in origin, suggesting that the Strelley Pool Chert kerogens may also be derived from diagenesis and thermal processing of biogenic organic matter. A combination of Raman spectroscopy, for identifying the least metamorphosed kerogens, used together with HyPy for liberating trapped and bound molecular components of these kerogens, offers a powerful strategy for assessing the origins of Earth's oldest preserved organic matter.

spectra obtained from ca. 1.8 Ga microfossils from the Gunflint Formation that are widely held to be biogenic although the authors could not rule out an abiogenic origin for Warrawoona organic matter particularly since they noted similarities in EELS and XANES spectra with Fischer Tropsch-synthesized carbons.

Westall and Rouzaud (2004) analyzed carbonaceous microfossils in 3.3–3.5 Ga cherts from Pilbara Craton and Barberton Greenstone Belts using TEM and Raman spectroscopy. The Raman spectrum was similar to that typically produced by disordered (but not amorphous) mature kerogen. HRTEM analysis revealed

NMR spectroscopy of carbonaceous materials isolated from the Strelley Pool Chert.

2. Geological setting

The Archaean Pilbara Craton, Western Australia, consists of three granite-greenstone terrains separated by late-tectonic clastic basins. The East Pilbara Granite-Greenstone Terrain represents the ancient nucleus of theraton. It consists of the 3.51–3.0 Ga Pilbara Supergroup of volcanic and sedimentary rocks that has been intruded by a variety of granitic rocks dated between 3.49 and 2.83 Ga (Figs. 1 and 2, Van Kranendonk et al., 2002, 2005). The Pilbara Supergroup consists of four autochthonous groups. The oldest (3.51–3.42 Ga)
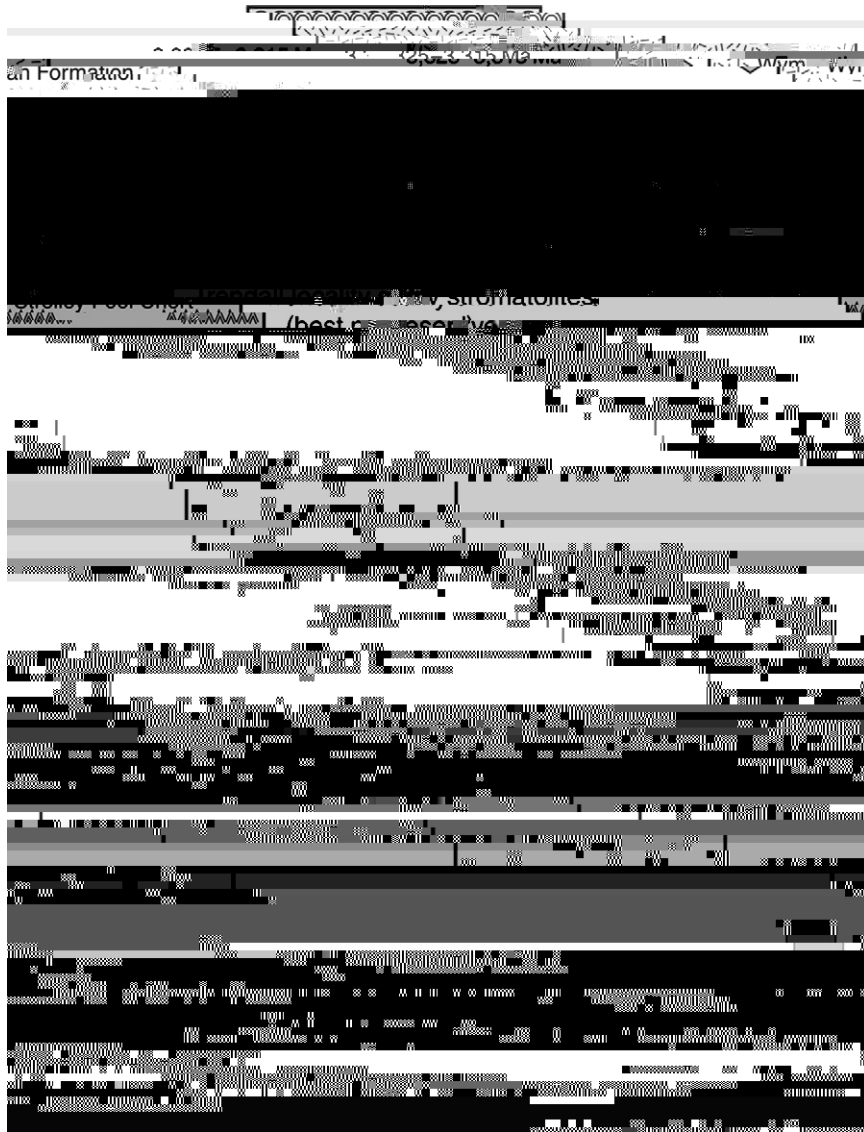
Fig. 2. Simplified stratigraphic column of the Warrawoona and Kelly Groups of the Pilbara Supergroup, showing the stratigraphic position of putative fossiliferous horizons, including the Strelley Pool Chert. See text for further description.

chert-barite units of the Dresser Formation that contain putative stromatolites and microfossils (Walter et al., 1980; Ueno et al., 2004); the Apex Basalt, which contains a chert unit that contains the controversial microfossils described by Schopf (1993) and Schopf et al. (2002), that have been contested by Brasier et al. (2002, 2005) and Garcia Ruiz et al. (2003) and putative microfossils in a thin chert unit in the Mount Ada Basalt (Awramik et al., 1983). These rocks were weakly deformed under low-grade metamorphic conditions and unconformably overlain by the ca. 3.43–3.32 Ga Kelly Group (Van Kranendonk et al., 2005), which consists of a basal chert-carbonate unit known as the Strelley Pool

Chert, and the conformably overlying Euro Basalt and Wyman Formation and Charteris Basalt. The Strelley Pool Chert, denoted as SPC, contains putative stromatolites deposited in a shallow marine environment (Lowe,

exciting laser beam, spectra were recorded from 2 to 10 different points in each sample to check the representative nature of the spectra. The Raman spectra were acquired on a Renishaw Raman Microprobe Laser Raman Spectrometer using a charge coupled detector. The collection optics are based on a Leica DMLM microscope. A refractive glass $50\times$ objective lens was used to focus the laser onto a 2 μm spot to collect the backscattered radiation. The 514.5 nm line of a 5 W Ar$^+$ laser (Spectra-Physics Stabilite 2017 laser)-mal to the sample was used to excite the sample. The instrument was calibrated against the Raman signal of Si at 520 cm^{-1} using a silicon wafer (1 1 1). Surface laser powers of 1.0–1.5 mW were used to minimize laser induced heating of the kerogens. An accumulation time of 30 s and 10 scans were used which gave adequate signal-to-noise ratio of the spectra. The scan ranges were 1000–1800 cm^{-1} in the carbon first-order region. The isolated kerogens were deposited as a dense layer of about 1 mm thickness, which was pressed with a steel spatula onto a clean aluminum microscope slide and irradiated with the laser to obtain spectra. For details regarding deconvolution and calculation of band areas refer to Allwood et al. (2006b).

3.7. Catalytic hydropyrolysis (HyPy)

The extracted kerogens were impregnated with an aqueous solution of ammonium dioxydithiomolybdate $[(NH_4)_2MoO_2S_2]$ to give a nominal loading of 2 wt.% molybdenum. Ammonium dioxydithiomolybdate reductively decomposes in situ under HyPy conditions above 250 °C to form a catalytically active molybdenum sulfide phase. HyPy runs were performed in an open-system temperature-programmed reactor configuration, which is described in detail previously (Love et al., 1995). In this investigation, the catalyst-loaded kerogens (200–600 mg) were initially heated in a stainless steel (316 grade) reactor tube from ambient temperature to 250 °C using a rapid heating rate of 300 °C min^{-1}, then to 520 °C at 8 °C min^{-1}, using a hydrogen gas pressure of 15 MPa. A constant hydrogen gas flow of 6 dm^3 min^{-1}, measured at ambient temperature and pressure, through the reactor bed ensured that the residence times of volatiles generated from pyrolysis were of the order of a few seconds. The HyPy products were collected in a silica gel trap cooled with dry ice. For comparison, a middle oil-window-mature Mesoproteozoic rock containing biogenic kerogen (core sediment from Urapunga4 well, 135.0–135.2 m depth, from ca. 1.45 Ga Velkerri Fm, Roper Group, McArthur Basin, Northern Territory, Australia, with Hydrogen

Index = 390 mg g TOC

and quantified to ensure that trace organic contamination levels were acceptably low.

3.8. Gas chromatography (GC) and gas chromatography–mass spectrometry (GC–MS)

Gas chromatography (GC) was performed with a Hewlett-Packard HP6890 gas chromatograph fitted with a flame ionization detector (FID) and a Chrompak CP Sil 5CB capillary column (60 m × 0.32 mm i.d., 0.25 μm film thickness) using He as a carrier gas. The GC oven was programmed at 60 °C (2 min), heated to 315 °C at 4 °C min^{-1}, with a final hold time of 25 min. Selected hydrocarbon products in total hydropyrolysates were quantified relative to the C_{22} branched alkane standard, 3-methylhenicosane, from relative peak areas.

Compound detection and identification was performed by GC–MS in full-scan mode on a Hewlett Packard HP6890 gas chromatograph interfaced to a Micromass AutoSpec Ultima magnetic sector mass spectrometer. GC separation was performed on a J&W Scientific DB-1MS capillary column (60 m × 0.25 mm i.d., 0.25 μm film thickness) using He as carrier gas. Samples were injected in splitless mode at 300 °C. The oven was programmed from 60 °C (held for 2 min) to 150 °C at 10 °C min^{-1}, then at 3 °C min^{-1} to 315 °C and held isothermal for 24 min. The source was operated in electron ionization (EI) mode at 70 eV ionization energy at 250 °C. The AutoSpec full-scan rate was 0.80 s/decade over a mass range of 50–600 Da and a delay of 0.20 s/decade. Peak identification was based on retention times and mass spectral comparisons with authenticated standards and well-characterized aromatic fractions of coal tar and crude oil (e.g., Kruge, 2000, and references therein).

3.9. Gas chromatography–isotope ratio mass spectrometry (GC–IRMS)

Compound-specific stable carbon isotopic compositions were measured on a Finnigan Delta + XL isotope-ratio-mass spectrometer coupled to an Agilent 6890 GC via the Finnigan combustion interface held at 850 °C with a constant oxygen trickle. Extracts were separated using a J&W DB-5 MS 30 m capillary column with 250 μm diameter and 0.25 μm film thickness. The oven temperature program for aromatic fractions was as follows: 40 °C (0.5 min) ramp to 90 °C at 20 °C min^{-1} (2 min hold) ramp to 290 °C at 3 °C min^{-1} then ramp to 320 °C at 20 °C min^{-1} (10 min hold). Samples were evaluated using injections of square peaks of CO_2 of known isotopic composition. Due to the complexity of the chromatograms external standards of known isotopic composition were used to estimate error. Error, reported as the root-mean-square error, for 16 individual n-alkanes was 0.23‰ for theses analysis. The pooled standard deviation for aromatic fractions was 0.75‰.

4. Results and discussion

4.1. Petrography

All samples except 1904-11 have a laminated fabric (Fig. 4A), which arises from the preferential alignment of sub-millimetre-sized carbonaceous clots and clasts in a matrix of polygonal microcrystalline quartz (Fig. 4B). The four laminated rock samples come from sedimentary beds and not from cross cutting (postdepositional) veins. The carbonaceous clots and clasts are part of the inherent rock fabric with clasts of silicified rocks or minerals, and the lamination defined
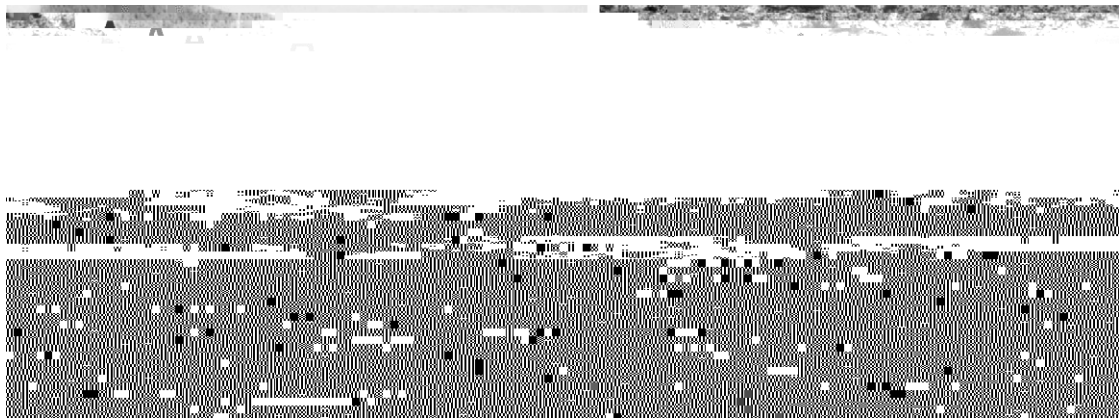

Fig. 4. Sedimentary fabric of representative sample thin sections. (A) Sample 120803-8: laminated fabric defined by the density and alignment of carbonaceous grains and particles in the chert matrix. Scale = 0.5 cm. (B) Sample 140803-2: carbonaceous material (black) occurring as clasts and clots distributed among rounded silicified grains, such as the large pale grain above centre.

by the carbonaceous clasts is continuous to the edges of the sample and is conformable with the larger sedimentary bedding. This attests to the syndepositional origin of the carbonaceous material. In contrast, sample 1904-11 comes from cross-cutting, post-depositional phreatomagmatic breccia matrix and displays no depositional layering. The carbonaceous material in 1904-11 occurs as evenly distributed clots and clasts in a chert matrix. The carbonaceous material in 1904-11 is therefore of post-depositional origin. No microfossils, like those described by Schopf (1993), were observed in our samples.

The kerogen isolated from all the chert samples is black, consistent with the samples having been subjected to a thermal history exceeding 250 °C (Hunt, 1996). This is in agreement with the thermal parameters derived in this study and from previous studies that show the SPC has been affected by post-depositional hydrothermal activity (Van Kranendonk and Pirajno, 2004).

4.2. TOC and elemental analysis

The total organic carbon (TOC) contents of the chert samples are low and vary from 0.08 to 0.22 wt.% (Table 1). Bulk atomic H/C ratios for isolated kerogens vary from 0.02 to 0.46 (Table 1). For comparative purposes, terrestrial semianthracite coals have H/C ratios of ~0.5 and cores of five or six aromatic rings, while anthracites have H/C ratios of ~0.3 and comprise clusters of greater than 15 aromatic rings. The range in bulk atomic H/C ratios suggests a thermal history variation between the samples with the lower H/C ratios signifying that these have been more thermally altered. Not surprisingly, the most thermally altered sample (1904-11) is the one sample in which the organic matter is not syndepositional but is associated with a cross-cutting breccia matrix.

4.3. Bulk kerogen $\delta^{13}C$ measurements

The bulk isotopic $\delta^{13}C$ compositions of kerogens are summarized in Table 1. The bulk $\delta^{13}C$ values vary from −28.3 to −35.8‰. The kerogens from the SPC are depleted in ^{13}C to a degree typically ascribed to biological processes. Recently, h45.6([(C)-2-2959.6(T.08))]TJn

Table 1

The total organic carbon (TOC) contents of Strelley Pool Cherts together with atomic H/C, N/C ratios, and $\delta^{13}C$ measurements for the indigenous organic matter in the samples investigated in this study

Samples	TOC (wt%)	H/C	N/C	$\delta^{13}C$ (‰)
1904-11	0.22	0.02	–	−34.0
1904-16	0.17	0.14	0.02	−35.0
140603-5	0.13	0.33	–	−35.2
120803-5	0.08	0.46	–	−28.3
120803-8	0.21	0.08	–	−35.8

lower greenschist facies metamorphism and given that the samples have been buried for 3.4 Ga.

4.5. ^{13}C Nuclear magnetic resonance (NMR) spectroscopy

A representative solid state ^{13}C NMR spectrum acquired from the isolated kerogen is shown in Fig. 5.

This is a typical CP MAS ^{13}C solid state NMR spectrum acquired from thermally overmature kerogens, in which the spectra have been collected under long accumulation times, but still show poor signal to noise (S/N). The spectrum shows a resonance band from 100–150 ppm, centered at approximately 125 ppm that corresponds to the presence of aromatic carbons which may be protonated (linked to a hydrogen atom) or non-protonated (most probably carbon substituted), and which we will refer to in total as aromatic carbon. In addition to the main aromatic carbon resonance, a slight shoulder can be observed at approximately 150 ppm. This is attributed to oxygen substituted aromatic carbons such as phenols and phenyl ethers. At the lower frequencies between 0 and 90 ppm, there is one small resonance centered at approximately 65 ppm which could be one of two possibilities: the resonance is an artifact or the resonance could be assigned to the presence of methoxy (O–CH$_3$) sp^3 bonded carbon functional group. It is more likely that this resonance at 65 ppm is an artifact of spectral acquisition.

It is clear that, qualitatively, aromatic carbon is the greatest constituent in the macromolecular network of these kerogens. The fraction of aromatic carbon (f_a), measured in this investigation for our samples varies from 0.90 to 0.92 (i.e., 90–92% of total carbon is aromatic). These f_a values derived from the solid-state ^{13}C

NMR (CP MAS) spectra are what would be expected given the H/C ratios obtained (0.02–0.46) from these samples. The H/C ratio's <0.5 suggest that the macromolecular network consists of very large PAH clusters on average (>15 aromatic rings), which is in agreement with the f_a values. Furthermore, these f_a values
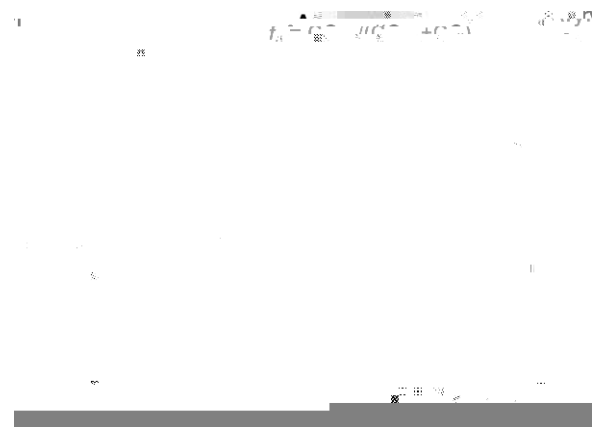

Fig. 5. A representative solid state ^{13}C NMR spectrum acquired from the isolated insoluble carbonaceous material (sample 120803-8).
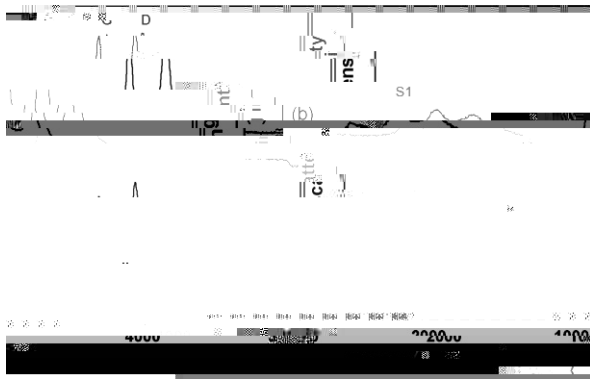
Fig. 6. Stacked Raman spectra are shown for the carbonaceous material isolated from (a) 1904-11 and (b) 120803-8, which shows pronounced absorptions at 1350 (D band) and $1600\,cm^{-1}$ (G band which is a combination of the G and D′ bands) in the first-order region and the second-order region contains a non intense S1 band at $2700\,cm^{-1}$. Note the D band intensity is greater for the spectrum acquired from 1904-11.

which is shown by the low band intensity in the second-order region (Lespade et al., 1982). Therefore, isolated kerogen from the SPC consists of small crystallites with biperoidic structure.

Minor differences in the intensities of the D band with respect to the G band can be observed for the two spectra. The D band intensity increases relative to the G band intensity, and the intensity of the D4 band gradually declines. These changes may reflect the increasing enlargement of polyaromatic structures and accompanying loss of peripheral hydrogen, which occurs during the conversion of polyaromatic structures to graphite (Negri et al., 2002). The width and relative band areas of the G and D lines vary with structural evolution and thus, can be used as an index of metamorphic alteration (e.g., Wopenka and Pasteris, 1993; Jehlicka et al., 2003; Beyssac et al., 2002, 2003; Quirico et al., 2005 and references therein). It can be noted that the spectrum acquired from the isolated kerogen from sample 1904-11 has a greater intensity of the D band, which corresponds to a more severe thermal history. The band becomes progressively narrow and increases in height relative to the G band, where upon increasing thermal maturity the D band decreases again, whereas the S bands increase in intensity representing the graphitization of organic matter. The Raman spectra obtained from these samples reveals that the kerogen has a low degree of 2-D structural organization and can be compared with other spectra of carbonaceous material taken from chlorite up to biotite metamorphic zones (e.g., Wopenka and Pasteris, 1993; Jehlicka et al., 2003 and references therein) representing lower to mid Greenschist facies (Yui et al., 1996),

carbonaceous materials; the higher the ratio, the greater the degree of structural disorder. $I_{D1}/(I_{D1} + I_G)$ values ranging from 51.8 to 57.8%, as measured in this investigation, indicate structurally disordered carbonaceous material. The dimensions of the graphitic domains or polyaromatic cluster size (L_a) range from 32.1 to 41.1 nm (Table 2) which would suggest the graphitic domains in these carbonaceous materials involve approximately 15–25 PNA units.

The ranges between the Raman parameters delineate a thermal trend between the samples. It can be observed from the H/C ratios (Table 1), I_{D1}/I_G, $I_{D1}/(I_{D1} + I_G)$, and L_a (Table 2) that a thermal trend can be delineated from most to least altered: 1904-11, 1904-16, 120803-8, 140603-5, and 120803-5. Fig. 7 shows cross-plots of H/C atomic ratios versus I_{D1}/I_G, $I_{D1}/(I_{D1} + I_G)$, and L_a. These cross-plots illustrate correlations between Raman parameters of measuring structural disorder of the macromolecular network (I_{D1}/I_G and $I_{D1}/(I_{D1} + I_G)$), and diameter of crystallite domains (L_a), with H/C atomic ratios.

The carbon first-order spectra for these isolated kerogens are typical spectra obtained from disordered sp^2 carbons, and have a similar line-shape to the spectra acquired by Brasier et al. (2002, 2005). The results and subsequent interpretation clearly show that the organic matter in the Warrawoona cherts are not graphitic as previously reported but are formed of nanometric polyaromatic domains. These results are also in agreement with those reported by Rouzaud et al. (2005). Geochemical maturation or metamorphism of almost all naturally occurring organic matter, whether biological or abiological (e.g., alkanes synthesized from FTT processes) in origin, has been proposed to give rise to similar resultant thermally stable products—covalently crosslinked aromatic hydrocarbons and other aromic subunits that that get transformed and condensed through carbonization and graphitization (Lindsay et al., 2005). So, Raman spectroscopy of over-mature carbonaceous material cannot provide definitive evidence of biogenicity by itself (Pasteris and Wopencka, 2003).

4.7. Catalytic hydropyrolysis (HyPy)

Fig. 8 displays representative TICs (Total Ion Chromatograms) of polyaromatic hydrocarbon (PAH) fractions prepared from hydropyrolysates for samples SPC 1904-11 and 1904-16. For these samples, an initial HyPy treatment up to 330

Table 4
Compound-specific stable carbon (δ^{13}C) isotopic composition (‰ vs. PDB) of selected aromatic compounds released from high temperature HyPy of Strelley Pool kerogens 1904-11 and 1904-16 as determined by GC–IRMS analysis

Sample	Kerogen	BiPh	MeAceN[a]	P	FlA	Py	BNfur
1904-11	−34.0	n.d.	n.d.	−32.9 (0.04)	−31.4 (1.31)	−35.8 (0.12)	n.d.
1904-16	−35.0	−29.3 (0.21)	−31.0 (0.47)	−30.5 (0.55)	−29.6 (0.85)	−32.9 (0.16)	−31.1 (0.32)

BiPh, 1,1′-biphenyl; MeAceN, methyacenaphthenes; P, phenanthrene; FlA, fluoranthene; Py, pyrene; BNfur, benzonaphthofuran. Values in parentheses indicate standard deviation from 2 or more analyses.

[a] Average of two resolvable peaks.

(7-ring PAH) coronene. While aromatic compounds of up to 7-ring PAH could be observed in hydropyrolysate of the 2 samples with highest H/C ratio (120803-5 and 140603-5) only 1–5 ring PAH could be produced for the more recalcitrant kerogens (1904-11, 1904-16 and 120803-8). The total PAH profiles for SPC and Urapunga4 kerogens exhibit the same characteristic features (Fig. 10) and are similar to, allowing for relative thermal maturity differences, the aromatic hydrocarbon distributions reported previously from HyPy of other mature Mesoproterozoic Roper Group kerogens (Brocks et al., 2003) and overmature late Archaean (ca. 2.5–2.7 Ga) marine kerogens from the Hamersley Province, Pilbara Craton (Brocks et al., 2003; Eigenbrode, 2004). The thermally less mature Urapunga4 aromatics, not surpris-
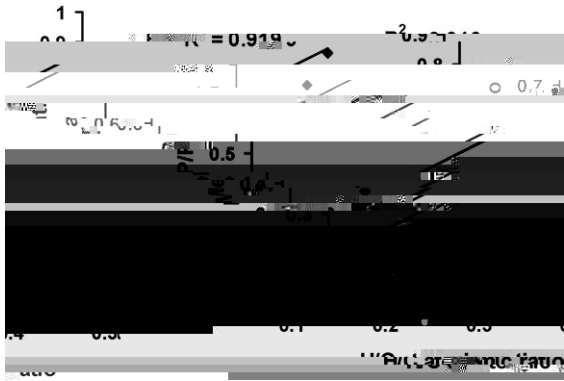
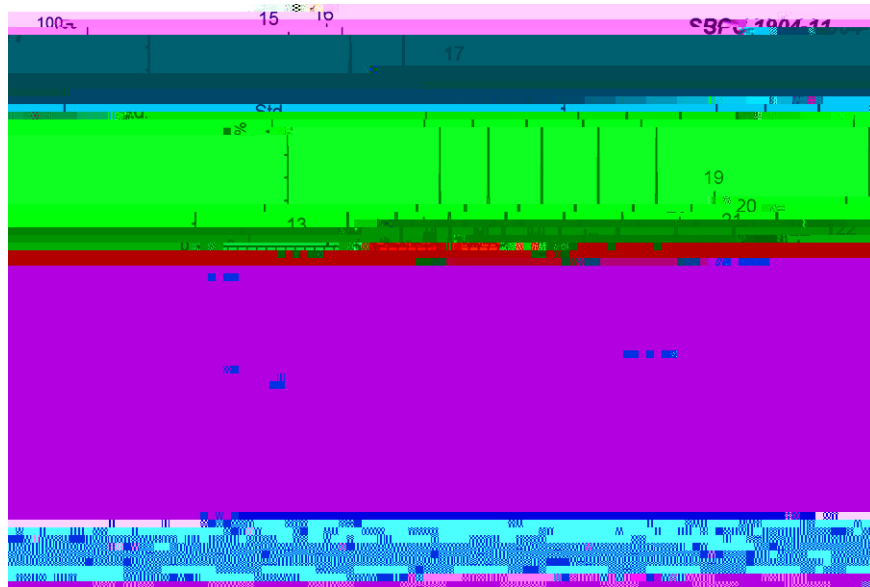Fig. 12. Cross-plot of atomic H/C atomic ratio vs. the molecular

Fig. 14. m/z 85 ion chromatograms for SPC 1904-11 and Urapunga4 (Mesoproterozoic) HyPy products, showing similar distributions of n-alkanes and methyl-branched alkanes (MMAs). Numbers (13–25) refer to the carbon chain length of n-alkanes. Not surprisingly, the n-alkane profiles for the less mature Urapunga4 sample extend to higher carbon numbers, although this may be at least partially a source effect.

fied even in very low levels relative to n-alkanes by m/z 83 or 97 ion chromatograms) for SPC HyPy products supports this interpretation. The alkanes released from SPC kerogens are unlikely to be contaminants because they are largely (>70 wt.%, Table 3) generated in the high T HyPy step and they exhibit an unusual mature alkane distribution unlike typical Phanerozoic petroleum fluids. A similar carbon number distribution of alkylcyclohexanes (m/z 83) and methylalkylcyclohexanes (m/z 97) is observed as for n-alkanes and supports the likeli-
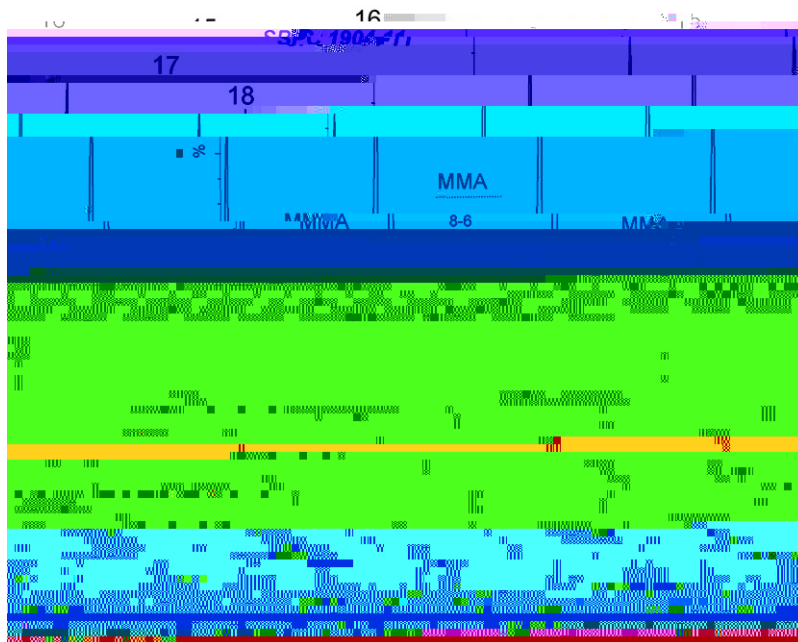

Fig. 15.[(Fig.)-243.4(15.).-8nce([(Fig.)-243.Ms4.7(stion)-11t(el1 0 T15(yl7.9701 8357byri.5(ch5CMf0.5 0 TD[(-alk[(Ftend)-250.1(iel1 0 T156b7Tf6bg45j/F1

spectral features are consistent with overmature and highly aromatic kerogen networks.

Obvious similarities are observed between molecular hydrocarbon profiles generated from catalytic hydropyrolysis (HyPy) of 5 Strelley Pool Chert kerogens (3.4 Ga)

restrial and extra-terrestrial carbons. Lunar and Planetary Science XXXVI, Abstract #1322.

Schidlowski, M., 2001. Carbon isotopes as biogeochemical reorders of life over 3.8 Ga of Earth history: evolution of a concept. Precambrian Res. 106, 117–134.

Schopf, J.W., 1993. Microfossils of the Early Arcean apex chert: new evidence of the antiquity of life. Science 260, 640–646.

Schopf, J.W., Kudryavtsev, A.B., Agresti, D.G., Wdowiak, T.J., Czaja, A.D., 2002. Laser-Raman imagery of Earth's earliest fossils. Nature 416, 73–76.

Sephton, M.A., Pillinger, C.T., Gilmour, I., 1999. Small-scale hydrous pyrolysis of macromolecular material in meteorites. Planet. Space Sci. 47, 181–187.

Sephton, M.A., Love, G.D., Watson, J.S., Verchovsky, A.B., Wright, I.P., Snape, C.E., Gilmour, I., 2004. Hydropyrolysis of insoluble carbonaceous matter in the Murchison meteorite: new insights into its macromolecular structure. Geochim. Cosmochim. Acta 68, 1385–1393.

Sephton, M.A., Love, G.D., Meredith, W., Snape, C.E., Sun, C.-G., Watson, J.S., 2005. Hydropyrolysis: a new technique for the analysis of macromolecular material in meteorites. Planet. Space Sci. 53, 1280–1286.

Sharp, T.G., De Gregorio, B.T., 2003. Determining the biogenicity of residual carbon within the Apex Chert. In: The Geological Society of America (GSA), 2003 Seattle Annual Meeting, November 2–5 (Paper No. 187-2).

Skrzypczak, A., Derenne, S., Robert, F., Binet, L., Gourier, D., Rouzaud, J.N., Clinard, C., 2004. Characterization of the organic matter in an Archean chert (Warrawoona, Australia). Geochim. Cosmochim. Acta 68, A240.

Skrzypczak, A., Derenne, S., Binet, L., Gourier, D., Robert, F., 2005. Characterization of a 3.5 Billion year old organic matter: Electron paramagnetic resonance and pyrolysis GC–MS, tools to assess syngeneity and biogenicity. Lunar and Planetary Science XXXVI, Abstract #1351.

Skrzypczak, A., Derenne, S., Robert, F., 2006. Molecular evidence for life in the 3.46 Ba-old Warrawoona chert. Geophys. Res. Abstr. 8, 06203 (EGU06-A-06203).

Stalker, L., Bryce, A.J., Andrew, A.S., 2005. A re-evaluation of the carbon isotopic composition of organic reference materials. Org. Geochem. 36, 827–834.

Tuinstra, F., Koenig, J.L., 1970. Raman spectra of graphite. J. Chem. Phys. 53, 1126–1130.

Ueno, Y., Isozaki, Y., Yurimoto, H., Maruyama, S., 2001a. Carbon isotopic signatures of individual Archaean microfossils (?) from Western Australia. Int. Geol. Rev. 43, 196–212.

Ueno, Y., Isozaki, Y., Yurimoto, H., Maruyama, S., 2001b. Early Archean (ca. 3.5) microfossils and 13C-depleted carbonaceous matter in the North Pole area, Western Australia. Field occurrence and geochemistry. In: Nakashima, S., Maruyama, S., Brack, A., Windley, B.F. (Eds.), Geochemistry and the Origin of Life. Universal Academy Press, pp. 203–236.

Ueno, Y., Yurimoto, H., Yoshioka, H., Komiya, T., Maruyama, S., 2002. Ion microprobe analysis of graphite from ca. 3.8 Ga meta-sediments, Isua supracrustal belt, West Greenland: Relationship between metamorphism and carbon isotopic composition. Geochim. Cosmochim. Acta 45, 1257–1268.

Ueno, Y., Yoshioka, H., Maruyama, S., Isozaki, Y., 2004. Carbon isotopes and petrography of kerogens in ∼3.5 Ga hydrothermal silica dikes in the North Pole area, Western Australia. Geochim. Cosmochim. Acta 68, 573–589.

Van Kranendonk, M.J., 2000. Geology of the NORTH SHAW